

# The hard-core model on planar lattices: the disk-packing problem and high-density phases

A. Mazel<sup>1</sup>, I. Stuhl<sup>2</sup>, Y. Suhov<sup>2,3</sup>

## Abstract

We study dense packings of disks and related Gibbs distributions representing high-density phases in the hard-core model on unit triangular, honeycomb and square lattices. The model is characterized by a Euclidean exclusion distance  $D > 0$  and a value of fugacity  $u > 0$ . We use the Pirogov-Sinai theory to study the Gibbs distributions for a general  $D$  when  $u$  is large:  $u > u_0(D)$ . For infinite sequences of values  $D$  we describe a complete high-density phase diagram: it exhibits a multitude of co-existing pure phases, and their number grows as  $O(D^2)$ . For the remaining values of  $D$ , except for those with sliding, the number of co-existing pure phases is still of the form  $E(D) \geq O(D^2)$ ; however, the exact identification of the pure phases requires an additional analysis. Such an analysis is performed for a number of typical examples, which involves computer-assisted proofs. Consequently, for all values  $D > 0$  where sliding does not occur, we establish the existence of a phase transition.

The crucial steps in the study are (i) the identification of periodic ground states and (ii) the verification of the Peierls bound. This is done by using connections with algebraic number theory. In particular, a complete list of so-called sliding values of  $D$  has been specified. As a by-product, we solve the disk-packing problem on the lattices under consideration. The number and structure of maximally-dense packings depend on the disk-diameter  $D$ , unlike the case of  $\mathbb{R}^2$ .

All assertions have been proved rigorously [26, 27], some of the proofs are computer-assisted.

## 1 Introduction

**1.1.** In this paper we report some rigorous results about the spherical hard-core (H-C)<sup>\*)</sup> model on planar lattices where the admissible configurations are packings of hard disks

---

2010 *Mathematics Subject Classification*: primary 60G60, 82B20, 82B26, 52C15

*Key words and phrases*: hard-core model, exclusion distance, Gibbs distributions, high-density/large fugacity, unit planar lattices, Pirogov-Sinai theory, dense-packing of disks, sliding

<sup>1</sup> AMC Health, New York, NY, USA; <sup>2</sup> Math Department, Penn State University, PA, USA; <sup>3</sup> DPMMS, University of Cambridge and St John's College, Cambridge, UK.

<sup>\*)</sup>For the reader's convenience, we provide the list of used abbreviations: H-C hard-core, GD Gibbs distribution, P-S Pirogov-Sinai, PGS periodic ground state, EGD extreme Gibbs distribution, AC admissible configuration, MDA maximally-dense admissible.

of diameter  $D$  representing particles with the Euclidean exclusion distance  $D$  and with centers at lattice sites.\*\*\*) Rigorous proofs of these results are contained in [26], [27].

When the fugacity/activity  $u > 0$  is small, the particle system is in a low-density/disordered phase; mathematically it means that in the thermodynamic limit the system has a unique *Gibbs distribution* (GD). An important question is how the system evolves when the density/fugacity increases, e.g., whether it undergoes phase transitions. In a high-density regime (where  $u$  is large) the H-C model is intrinsically related to the optimal (i.e., maximally-dense) disk-packing problem on the underlying lattice. Here the system is expected to become ordered, i.e., to be in a crystalline/solid phase (one or several). We show that this fact holds true in the thermodynamic limit for all but finitely many explicitly enumerated values of  $D$ , provided that  $u$  is large enough:  $u \in (u_0, \infty)$  where  $u_0$  depends on  $D$  and the type of the lattice under consideration. The excluded values of  $D$  exhibit a phenomenon of sliding defined and described in section 3.3. For all non-sliding values of  $D$  we give a description of the large-fugacity phase diagram establishing that the pure phases always emerge from optimal/maximally dense disk-packing configurations (ground states), but not necessarily from all of them. Such non-uniqueness of pure phases proves the existence of a phase transition for all non-sliding values of  $D$  [15], [16]. The structure of ground states is analyzed in number-theoretical and geometric terms.

We consider unit triangular, honeycomb and square lattices,  $\mathbb{A}_2$ ,  $\mathbb{H}_2$  and  $\mathbb{Z}^2$ . It turns out that only *attainable* values of  $D$  (or rather  $D^2$ ) are of interest, i.e., those that can be realized on the corresponding lattice. On  $\mathbb{A}_2$  and  $\mathbb{H}_2$  the attainable values  $D^2$  are of the form  $D^2 = a^2 + b^2 + ab$ , while on  $\mathbb{Z}^2$  they obey  $D^2 = a^2 + b^2$ , where  $a, b$  are non-negative integers. (For a non-attainable disk diameter  $D'$  one applies the results for the smallest attainable  $D$  such that  $D > D'$ .)

A complete description of the large fugacity phase diagram requires the determination of all pure phases; mathematically it means an identification of *extreme Gibbs distributions* (EGDs). A popular tool here is the Pirogov-Sinai (P-S) theory [31], [36], based on (i) a specification of *periodic ground states* (PGSs) and (ii) verification of the *Peierls bound* for the statistical weight of a deviation of an admissible particle configuration from a PGS. For reviews of the P-S theory, cf. [12], [32], [33], [37]; for a general view in the context of statistical mechanics, see [5].

Lattice H-C models (with a variety of hard-core shapes) attracted a considerable interest in statistical mechanics, beginning with [6], [8], [13], [14]. Thereupon, an extensive mathematical and physical bibliography has been generated (including experimental studies of specific materials); cf. [1] - [4], [9], [11], [18], [20], [22], [23], [29], [30], [34] and references therein.

The existence of multiple EGDs in a high-density regime has been rigorously proved (i) in [8] on  $\mathbb{Z}^d$  for  $D = \sqrt{2}$  (for all  $d > 1$ ), (ii) in [18] on  $\mathbb{A}_2$  for a family of values  $D$  and (iii) for a class of H-C lattice particle systems in [23]. In relation to the spherical H-C model on  $\mathbb{A}_2$ ,  $\mathbb{H}_2$  and  $\mathbb{Z}^2$ , our work includes these results as partial cases of a general theory.

An exact solution for a spherical H-C model was obtained for  $D^2 = 3$  on the triangular lattice  $\mathbb{A}_2$  [3], [4].

For some of the sliding values of  $D$  on  $\mathbb{Z}^2$ , paper [30] states the existence of a columnar

---

\*\*)The value  $D$  gives the minimal allowed distance at which the centers of disks can be placed.

order; for the sliding value  $D = 2$  the presence of a columnar order has been proven in [17].

Spherical H-C models on two-dimensional lattices gained a growing popularity in the recent physical literature [1], [9], [11], [20], [29], [30], [34] and references therein. Most of these papers specify the model as  $k$ -nn or  $k$ -NN exclusion, indicating that a particle excludes all nearest-neighboring sites, 2-nd nearest-neighboring sites, ...,  $k$ -th nearest-neighboring sites (all in the planar Euclidean metric). The value  $D$  used to specify the model in the current paper is the Euclidean distance to the  $(k + 1)$ -st nearest-neighbors. A subject of interest is that, depending on the lattice type and the value of  $D$ , one expects different forms of phase transitions when the particle density/fugacity/chemical potential in the system increases. A progress in simulation and analytical techniques led to predictions for critical points and types of the related phase transitions for some initial values of  $k$ . For H-C models on  $\mathbb{Z}^2$  we refer to [11], [29], [30], on  $\mathbb{A}_2$  to [1], [20], and on  $\mathbb{H}_2$  to [9], [34].

Our work considers all values of  $k \in \mathbb{N}$  and analyzes the model in the thermodynamic limit. We give a detailed description of optimal/maximally-dense packings and – for the cases without sliding – of their associated large-fugacity phases. Our findings regarding the large-fugacity pure phases coincide with those obtained in [2], [9], [20], [29] and [34] for initial values of  $k$  considered therein. However, a rigorous analysis of criticality remains an open (and challenging) mathematical problem.

**1.2.** A brief summary of our results is as follows. On each of the lattices  $\mathbb{Z}^2$ ,  $\mathbb{A}_2$  and  $\mathbb{H}_2$ , the set of attainable values of  $D$  is partitioned into three distinct groups (A)–(C) characterized by different structures of extreme Gibbs distributions. (A) For some explicitly determined infinite sequences of numbers  $D$  we provide a complete picture of the set of the large fugacity EGDs. It yields a multitude of co-existing pure phases where every periodic ground state generates an EGD. The number  $E(D)$  of the EGDs grows as  $O(D^2)$ . (B) For the remaining infinite sets of values  $D$ , except for 39 particular numbers on  $\mathbb{Z}^2$  and 4 on  $\mathbb{H}_2$ , there is still a multitude of coexisting pure phases, with  $E(D)$  growing at least as  $O(D^2)$ , but not all PGSs generate EGDs. Here the problem is reduced to an identification of *dominant* PGSs (see section 5.1). The corresponding complete analysis has been done in [26] for a selection of typical examples. (C) For the 43 excluded values of  $D$  the model exhibits a phenomenon of *sliding* (see section 3.3).

For a value  $D$  from group (A) there is a finite number of PGSs, and any two of them are taken to each other by an underlying lattice symmetry. Consequently, if one of these PGSs generates an EGD then so does each of them, and all generated EGDs are distinct. For a value  $D$  from group (B) there are at least two symmetry classes of PGSs. PGSs from a given class are taken into each other by a lattice symmetry, but any two representatives of different symmetry classes are not lattice-symmetric to each other. Typically, only PGSs from one symmetry class generate EGDs; for that reason such a class and the PGSs in it are called *dominant*. For values  $D$  from group C there is an infinite degeneracy of PGSs; typically these PGSs are layered configurations consisting of 1-dimensional layers. Moreover, each of these layers can be placed in at least two different positions independently of the positions of other layers, and all obtained configurations remain ground states. This represents a phenomenon of sliding in the two-dimensional H-C models under consideration. Note that a phenomenon of sliding exists in H-C models

in higher dimensions as well although its precise definition is more involved.

**1.3.** In the course of identifying ground states we solve the disk-packing problem on  $\mathbb{A}_2, \mathbb{H}_2$  and  $\mathbb{Z}^2$ . Namely, given an attainable  $D^2$ , we establish the supremum of the disk-packing density among all packings/admissible configurations, both periodic and non-periodic, and show that it is achievable.

Let  $\mathbb{W} = \mathbb{A}_2, \mathbb{H}_2, \mathbb{Z}^2$  and  $\Lambda_l$  be a square of side-length  $l$  on  $\mathbb{R}^2$ . We define the maximal disk-packing density by

$$\delta(D, \mathbb{W}) := \sup_{\Phi} \left\{ \limsup_{l \rightarrow \infty} \frac{\text{Area}(\Phi \cap \Lambda_l)}{\text{Area}(\Lambda_l)} \right\},$$

where  $\Phi$  is a packing of disks of diameter  $D$  with centers at sites of  $\mathbb{W}$ .

It turns out that for any attainable  $D^2$  on  $\mathbb{A}_2$  and any attainable  $D^2$  on  $\mathbb{H}_2$  divisible by 3,

$$\delta(D, \mathbb{A}_2) = \delta(D, \mathbb{H}_2) = \frac{\pi}{2\sqrt{3}},$$

which gives the maximal disk-packing density on  $\mathbb{R}^2$ . Dense-packings on  $\mathbb{A}_2$  have been considered in [7] as well.

Next, for all attainable  $D^2$  on  $\mathbb{H}_2$  non-divisible by 3, except for  $D^2$  from the collection  $\mathcal{N} := \{1, 4, 7, 13, 16, 28, 31, 49, 64, 67, 97, 133, 157, 256\}$ , the maximal disk-packing density has the form

$$\delta(D, \mathbb{H}_2) = \frac{\pi D^2}{2\sqrt{3}(D^*)^2}.$$

Here  $D^* > D$  is the closest attainable value with  $(D^*)^2$  divisible by 3. Finally, for  $D^2 \in \mathcal{N}$ , the identification of the dense-packings on  $\mathbb{H}_2$  is done case-by-case, and we refer the reader to [26] for their detailed description. These configurations consist of periodically alternating triangular tiles of two distinct types, not necessarily forming a sub-lattice.

On the other hand, for all attainable  $D$  on  $\mathbb{Z}^2$

$$\delta(D, \mathbb{Z}^2) = \frac{\pi D^2}{4S(D)},$$

where  $S(D)/2$  is the solution to optimization problem (5); see below.

Furthermore, for any attainable non-sliding  $D$  on  $\mathbb{A}_2, \mathbb{H}_2, \mathbb{Z}^2$  we describe all periodic optimizers, i.e., periodic packings achieving the maximal density. On  $\mathbb{A}_2$  these are  $D$ -sub-lattices and their shifts (see section 3.2), while on  $\mathbb{Z}^2$  they are the so-called maximally-dense admissible sub-lattices and their shifts (see section 3.5). On  $\mathbb{H}_2$  the optimizers are  $D$ -sub-lattices and their shifts when  $D^2$  is divisible by 3, and  $D^*$ -sub-lattices and their shifts when  $D^2 \notin \mathcal{N}$  and  $D^2$  is not divisible by 3 (see section 3.4). For  $D^2 = 1, 13, 16, 28, 49, 64, 67, 97, 157, 256$  on  $\mathbb{H}_2$  there are finitely many optimal periodic packings but they are not necessarily sub-lattices: cf. [26]. For the 43 sliding values  $D$  (on  $\mathbb{Z}^2$  and  $\mathbb{H}_2$ ), we construct infinitely many optimal periodic packings.

We would like to note that, for each of  $\mathbb{A}_2, \mathbb{Z}^2$  and  $\mathbb{H}_2$ , there are infinitely many values of  $D$  for which the optimizer is unique up to lattice symmetries, and there are also infinitely many values of  $D$  with multiple, but finitely many, optimizers up to lattice

symmetries. Moreover, these alternatives exhaust all attainable non-sliding values of  $D$ . The number of optimal packings depends upon  $D$ ; on  $\mathbb{Z}^2$  and  $\mathbb{H}_2$  the disks in these packings do not necessarily touch their ‘neighbors’.

## 2 Gibbs distributions

**2.1.** A  $D$ -admissible configuration ( $D$ -AC) on  $\mathbb{W}$  is a map  $\phi : \mathbb{W} \rightarrow \{0, 1\}$  such that  $\text{dist}(x, y) \geq D$ , for all  $x, y \in \mathbb{W}$  with  $\phi(x) = \phi(y) = 1$ . Sites  $x \in \mathbb{W}$  with  $\phi(x) = 1$  are treated as occupied, those with  $\phi(x) = 0$  as vacant. The set of  $D$ -ACs is denoted by  $\mathcal{A} = \mathcal{A}(D, \mathbb{W})$ . Similar definitions can be introduced for a subset  $\mathbb{V} \subseteq \mathbb{W}$ . Cf. Fig. 1. Given  $\mathbb{V} \subseteq \mathbb{W}$ , we say that configuration  $\psi \in \mathcal{A}(D, \mathbb{V})$  is compatible with  $\phi \in \mathcal{A}$  if the concatenation  $\psi \vee (\phi|_{\mathbb{W} \setminus \mathbb{V}}) \in \mathcal{A}$ . Define the probability distribution  $\mu_{\mathbb{V}}(\cdot || \phi)$  on  $\mathcal{A}(D, \mathbb{V})$ :

$$\mu_{\mathbb{V}}(\psi || \phi) := \begin{cases} \frac{u^{\sharp\psi}}{Z(\mathbb{V} || \phi)}, & \psi \text{ is compatible with } \phi, \\ 0, & \text{otherwise.} \end{cases} \quad (1)$$

Here  $\sharp\psi$  stands for the number of occupied sites in  $\psi \in \mathcal{A}(D, \mathbb{V})$  and  $Z(\mathbb{V} || \phi)$  is the partition function in  $\mathbb{V}$  with the boundary condition  $\phi \in \mathcal{A}$ :

$$Z(\mathbb{V} || \phi) := \sum_{\psi \in \mathcal{A}(D, \mathbb{V})} u^{\sharp\psi} \mathbf{1}(\psi \text{ is compatible with } \phi). \quad (2)$$

$\mu_{\mathbb{V}}(\cdot || \phi)$  is called an H-C Gibbs distribution in ‘volume’  $\mathbb{V}$  with the boundary condition  $\phi$  at fugacity  $u > 0$ .

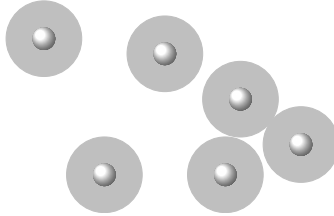


Figure 1: An admissible configuration

**2.2.** A modern mathematical definition describes a Gibbs distribution  $\mu$  on  $\mathbb{W}$  as a (Borel) probability measure concentrated on set  $\mathcal{A}$  and related to a (Gibbsian) *specification* formed by the family  $\{\mu_{\mathbb{V}_n}(\cdot || \phi)\}$ . Cf. [15], Chapter 2, particularly, Definition 2.9. Of a particular importance are extreme Gibbs distributions which cannot be written as a non-trivial mixtures of other GDs. In this paper we work with GDs obtained as thermodynamic limits in the Van Hove sense

$$\lim_{\mathbb{V}_n \nearrow \mathbb{W}} \mu_{\mathbb{V}_n}(\cdot || \phi) \quad (3)$$

in the weak topology. If it exists, the limiting measure in (3) is denoted by  $\mu_\phi$ , and we say that  $\mu_\phi$  is generated by  $\phi \in \mathcal{A}$ .

This work studies the H-C EGDs for values  $u$  large enough; such an assumption is in force throughout the paper and not stressed every time again. The structure of set  $\mathcal{E}(D)$  depends both on the choice of lattice  $\mathbb{W}$  and arithmetic properties of  $D$  and is studied using the P-S theory based on the notion of a PGS.

A ground state is defined as a  $D$ -AC  $\varphi \in \mathcal{A}$  with the property that one cannot remove finitely many particles from  $\varphi$  and replace them by a larger number of particles without breaking admissibility. A PGS is a ground state invariant under two non-collinear lattice shifts, hence under their convolutions. A parallelogram spanned by the corresponding vectors is called a period of a PGS. We let  $\mathcal{P}(D) = \mathcal{P}(D, \mathbb{W})$  denote the set of PGSs for given  $D$  and  $\mathbb{W}$ .

The P-S theory [31], [36], states that, under certain assumptions, (a) every periodic EGD  $\mu$  is generated by a PGS  $\varphi$  in the sense of (3):  $\mu = \mu_\varphi$ , (b) every periodic EGD  $\mu$  has a list of properties stressing its pure-phase character (see items **(P1)**–**(P5)** in section 5.1.), (c) there are no other periodic EGDs. Moreover, general results from [10] ensure that in a wide class of two-dimensional models, including the H-C model, there is no non-periodic EGD at large fugacities, i.e., non-periodic ground states do not generate EGDs. Hence, indentifying the PGSs and applying the above-mentioned general results from [31], [36], [10], including the identification of dominant/stable PGSs, would allow one to describe all large-fugacity EGDs. The assumptions from [31], [36], [10] that we need to verify are that **(I)** there are finitely many PGSs, and **(II)** a deviation from a PGS is controlled by a suitable Peierls bound based on an appropriate notion of a *contour*. Verifying these assumptions is a key part of this work.

### 3 Periodic ground states

**3.1.** Let us consider assumption **(I)**. It turns out that, apart from a few exceptional values of  $D$  on  $\mathbb{H}_2$  and  $\mathbb{Z}^2$  which have to be analyzed separately, the PGSs on  $\mathbb{W} = \mathbb{A}_2, \mathbb{H}_2, \mathbb{Z}^2$  are given by *maximally-dense admissible* (MDA) sub-lattices  $\mathbb{E} \subset \mathbb{W}$  and their  $\mathbb{W}$ -shifts. This is a non-trivial result established in [26, 27]. In the simplest cases an MDA sub-lattice arises because an admissible triangle of minimal area uniquely tessellates the corresponding lattice, up to lattice symmetries and shifts. (Cf. Theorem I in [26], Lemma I and Theorem 1 (i) in [27]). A non-unique tessellation by a given minimal area triangle always leads to sliding (section 2.2 in [27], section 8 in [26]).

Furthermore, on  $\mathbb{H}_2$  there are cases where no admissible triangle of minimal area tessellates the whole lattice. In the majority of these cases (constituting an infinite amount of values of  $D$ ), an additional number-theoretical argument verifies that PGSs are still given by MDA sub-lattices (Theorem 1 (ii), Lemma 4.10 (cases  $D^2 = 64, 67$ ) in [26]). Among the remaining cases there are values of  $D$  for which some of the corresponding PGSs are not MDA sub-lattices. (Theorem 1 (ii), Lemma 4.10 (all cases except for  $D^2 = 64$ )).

Observe that in all cases one can construct non-periodic ground states, e.g., by filling two half-planes with different PGSs. Additional clarifications are provided in section 3.6.

The  $\mathbb{W}$ -shifts and  $\mathbb{W}$ -symmetries ( $\mathbb{W}$ -reflections/rotations) define a partition of set  $\mathcal{P}(D, \mathbb{W})$  into PGS-*equivalence classes*. Let  $K = K(D, \mathbb{W})$  denote the number of PGS-equivalence classes. Recall that, by the definition of sliding, if  $D$  is non-sliding then



$K < \infty$ . For a case when  $D$  is non-sliding and on  $\mathbb{W} = \mathbb{H}_2$  when  $D^2 \notin \mathcal{N}$  a PGS is always an MDA sub-lattice or its shift. Let  $\sigma$  stand for the number of lattices sites in the half-open fundamental parallelogram of an MDA-sub-lattice and  $m_j$  denote the number of distinct MDA-sub-lattices within a given PGS-equivalence class, for  $j = 1, \dots, K$ . Then, for the cardinality  $\#\mathcal{P}(D, \mathbb{W})$  of the set of PGSs  $\mathcal{P}(D, \mathbb{W})$  we have

$$\#\mathcal{P}(D, \mathbb{W}) = \sigma \sum_{j=1}^K m_j. \quad (4)$$

Further specifications for  $K$ ,  $\sigma$  and  $m_j$  depend on the choice of  $\mathbb{W}$  and  $D$  and are provided below. In particular, dependence upon  $D$  is non-monotonic and exhibits connections with the algebraic number theory.

**3.2.** On  $\mathbb{A}_2$ , for any  $D$  every MDA sub-lattice is obviously a  $D$ -sub-lattice, for which a fundamental parallelogram is formed by two equilateral triangles with side-length  $D$  ( $D$ -triangles). This is due to the fact that an equilateral triangular arrangement solves the dense-packing problem in  $\mathbb{R}^2$ . Consequently, on  $\mathbb{A}_2$  the value  $\sigma = D^2$ .

It is not hard to see that on  $\mathbb{A}_2$ , admissibility of  $D$  is equivalent to solvability of the Diophantine equation  $D^2 = a^2 + b^2 + ab$ ,  $a, b \in \mathbb{Z}$  (i.e., to the fact that  $D^2$  is a Lösschian number). Therefore, the number  $K$  of PGS-classes in Eqn (4) is directly related to the number of solutions  $a, b \in \mathbb{Z}$ ,  $0 \leq a \leq b$ , to this equation. It is well-known that a solution exists iff the prime decomposition of  $D^2$  contains primes of the form  $3v+2$  in even powers. See Proposition 9.1.4, [19].

We will consider three disjoint groups of values of  $D$  (or  $D^2$ ) deemed TA1, TA2 and TB, and based on further conditions upon prime factors of  $D^2$ . The first character in the labels TA1, TA2 and TB reflects the choice of a lattice (T stands for triangular). Derivation of these results based on known number-theoretical facts can be found in Theorems 1 - 3 from [26].

First, take the case TA1: here  $D^2$  is of the form  $D^2 = a^2$  or  $D^2 = 3a^2$  where  $a \in \mathbb{N}$  has only prime factors 3 or prime factors of the form  $3v+2$ , i.e., the prime decomposition of  $D^2$  has no primes of form  $3v+1$ . Then the above Diophantine equation has a unique solution, and the  $D$ -sub-lattice is  $\mathbb{A}_2$ -reflection invariant; consequently,  $K = 1$ ,  $m_1 = 1$  and the number of PGSs is  $D^2$ .

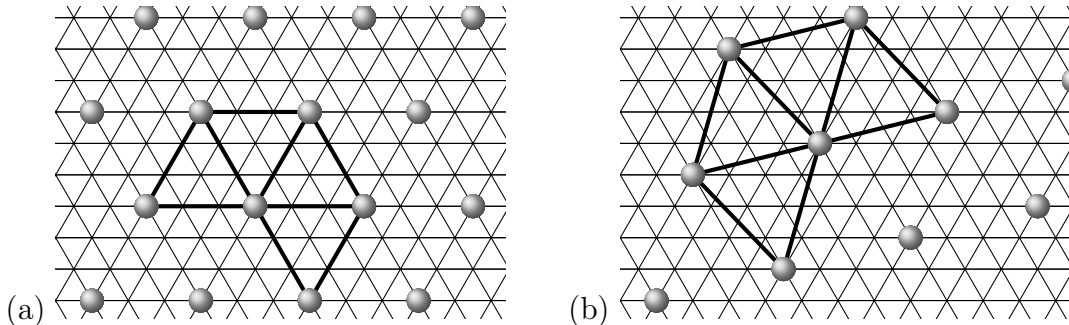


Figure 2: PGSs on  $\mathbb{A}_2$ , for  $D^2 = 9$  (Case TA1) (a), and  $D^2 = 13$  (Case TA2) (b). The number of PGSs is 9 and 26, respectively.

Case TA2 emerges when the equation has a unique solution such that  $a < b$ , with  $a, b \in \mathbb{N}$ . A value  $D^2$  belongs to the TA2 case iff its prime decomposition has a single prime of form  $3v + 1$ . In this case  $K = 1$ , the  $D$ -sub-lattice is not  $\mathbb{A}_2$ -reflection invariant,  $m_1 = 2$ , and the number of PGSs is  $2D^2$ . Cf. Fig. 2.

The 3rd case, TB, covers all remaining values of  $D$ ; in this case the equation has multiple solutions. Each solution  $a, b$ ,  $0 \leq a \leq b$ , generates a PGS-equivalence class, and its cardinality is  $D^2$  or  $2D^2$ , similarly to the above cases TA1 and TA2. Cf. Fig. 3.

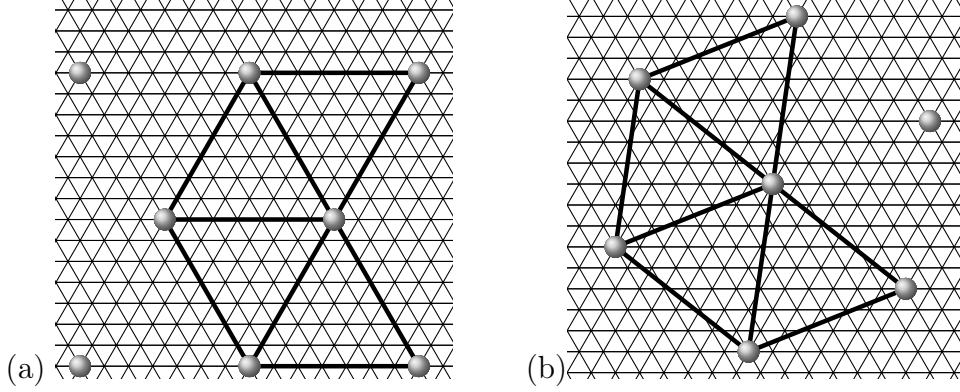


Figure 3: PGSs on  $\mathbb{A}_2$  for  $D^2 = 49$  (Case TB). There are 49 horizontal PGSs (a) and 98 inclined (b). The horizontal PGSs are the only dominant ones.

Classes TA1, TA2, TB form a partition of values of  $D$  on  $\mathbb{A}_2$ . Given  $D$  the knowledge of the corresponding class provides a specification of the number of PGSs and their structure.

**3.3.** Now consider  $\mathbb{W} = \mathbb{H}_2, \mathbb{Z}^2$ . As was said, for some values  $D^2$  on  $\mathbb{H}_2$  and  $\mathbb{Z}^2$  we encounter a phenomenon of sliding. It occurs when one can pass from one PGS to another without any local loss in ‘energy’ i.e., without decreasing the local particle numbers.

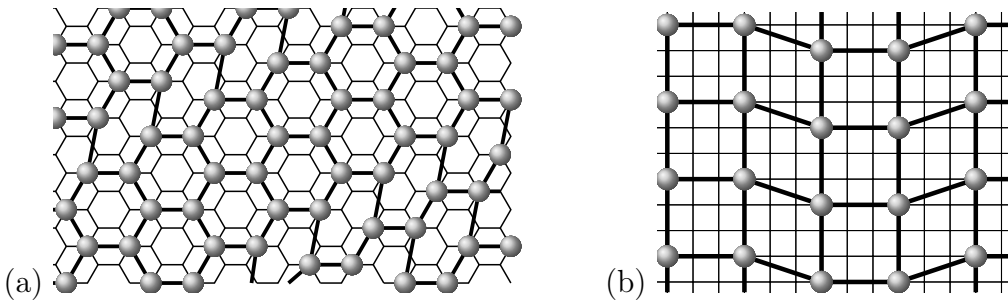


Figure 4: Sliding on  $\mathbb{H}_2$  for  $D^2 = 4$  (a) and on  $\mathbb{Z}^2$  for  $D^2 = 9$  (b).

On  $\mathbb{H}_2$  there are just 4 sliding values:  $D^2 = 4, 7, 31, 133$ ; the proof of this fact is computer-assisted [26]. Cf. Fig. 4 (a).

On  $\mathbb{Z}^2$  there exist 39 sliding values:  $D^2 = 4, 8, 9, 18, 20, 29, 45, 72, 80, 90, 106, 121, 157, 160, 218, 281, 392, 521, 698, 821, 1042, 1325, 1348, 1517, 1565, 2005, 2792, 3034, 3709, 4453, 4756, 6865, 11449, 12740, 13225, 15488, 22784, 29890, 37970$ . Cf. Fig. 4 (b).



This was first conjectured by the authors [27], then in [24] it was proved that the sliding list is finite, then finally the completeness of the above list was independently established in [27], [25]. A part of the list was identified in [30] as candidates for occurrence of a columnar order. In a recent paper [17], the case of  $D^2 = 4$  on  $\mathbb{Z}^2$  was rigorously analyzed, confirming existence of four EGDs with a columnar order.

In what follows we consider the non-sliding values of  $D$  only.

**3.4.** Additionally, on  $\mathbb{H}_2$  there are exceptional values  $D^2 = 1, 13, 16, 28, 49, 64, 97, 157, 256$  where the PGS-class is unique but is non-lattice. Cf. Fig. 5. Furthermore, for  $D^2 = 67$  there are two classes one of which is non-lattice. These values are analyzed via a special approach (see [26], Theorems 12, 13) and not discussed in this article.

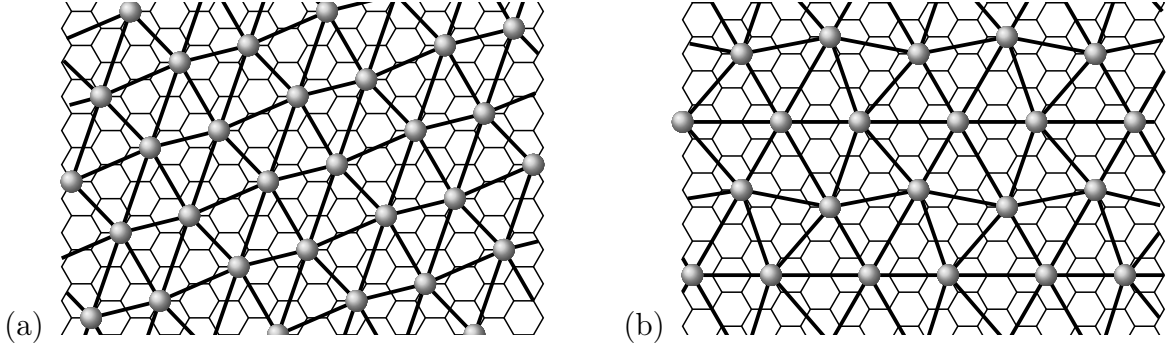


Figure 5: Non-lattice PGSs on  $\mathbb{H}_2$  for  $D^2 = 13$  (a) and  $D^2 = 16$  (b).

Thus, in what follows, on  $\mathbb{H}_2$  we refer to non-exceptional values of  $D$ : here every PGS is an MDA-sub-lattice. More precisely, if 3 divides  $D^2$  then every PGS is a  $D$ -sub-lattice since a  $D$ -triangle can be inscribed in  $\mathbb{H}_2$ . Accordingly, we define groups of values  $D^2$  deemed HA1, HA2 and HB and formed by the values from cases TA1, TA2 and TB divisible by 3. When  $D^2$  belongs to one of these H-cases, the theory goes in parallel to the respective T-case. See Theorems I (ii), 7, 8, 9 in [26]. In particular, this yields the same values  $K, m_k$  while  $\sigma = 2D^2/3$ . Cf. Fig. 6.

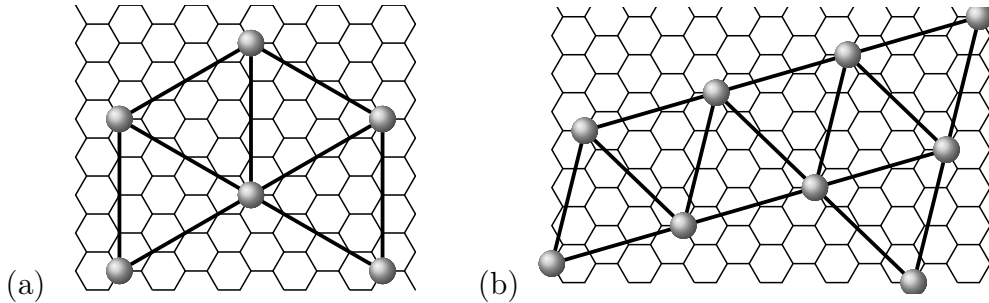


Figure 6: PGSs on  $\mathbb{H}_2$ , for  $D^2 = 48$  (Case HA1) (a), and  $D^2 = 39$  (Case HA2) (b). The number of PGSs is 32 and 52, respectively.

When  $D^2$  is not divisible by 3, we pick the nearest Lösschian number  $(D^*)^2 > D^2$  divisible by 3: the fact is that every MDA-sub-lattice is a  $D^*$ -sub-lattice in  $\mathbb{H}_2$ , as triangles

with area less than that of the  $D^*$ -triangle do not generate  $D$ -admissible PGSs. This defines a group of values  $D^2$  called case HC, for which the above theory is repeated with  $D$  replaced by  $D^*$ . See Theorems I (ii), 12 in [26]. Cf. Fig. 7.

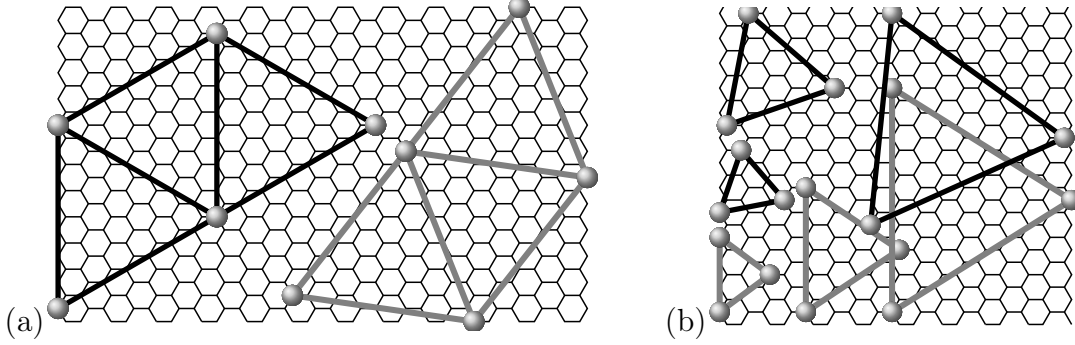


Figure 7: (a) PGSs on  $\mathbb{H}_2$  for  $D^2 = 147$  (Case HB). The ‘vertical’ PGSs (black) are dominant. (b) PGSs on  $\mathbb{H}_2$  for values  $D^2$  from Class HC, with  $D^{*2} = D^2 + 2$ , and their associated  $D^*$ -triangles (black). (i) For  $D^2 = 19$ ,  $D^{*2} = 21$ . (ii) For  $D^2 = 61$ ,  $D^{*2} = 63$ . (iii) For  $D^2 = 217$ ,  $D^{*2} = 219$ . The gray  $\mathbb{H}_2$ -triangles give the minimal area when the side-lengths are  $\geq D$  and the angles  $\leq \pi/2$ . However, they do not generate PGSs. The PGSs are MDA-lattices constructed from the black  $D^*$ -triangles.

**3.5.** A different situation emerges on  $\mathbb{Z}^2$ , where a  $D$ -triangle can never be inscribed. Nevertheless, every PGS-equivalence class is constructed from an MDA-sub-lattice. The MDA-sub-lattices in  $\mathbb{Z}^2$  are defined implicitly, via solutions of a discrete optimization problem

$$\begin{aligned} &\text{minimize the area of a } \mathbb{Z}^2\text{-triangle } \triangle \\ &\text{with one vertex at the origin,} \\ &\text{with side-lengths } \ell_i \geq D \text{ and angles } \alpha_i \leq \pi/2. \end{aligned} \tag{5}$$

The term  $\mathbb{Z}^2$ -triangle means a triangle with vertices in  $\mathbb{Z}^2$ . Accordingly,  $\sigma = S$  where  $S/2$  is the minimum achieved in (5). A minimizing triangle in (5) is referred to as an *M-triangle*. Adjacent pairs of M-triangles form fundamental parallelograms of MDA-sub-lattices generating the PGSs. Cf. Fig. 8.

Problem (5) always has a solution but the M-triangle  $\triangle$  may be non-unique. A delicate point is that there are different types of non-uniqueness of an M-triangle: (i) there are  $N_0 > 1$  M-triangles, and they are  $\mathbb{R}^2$ - but not  $\mathbb{Z}^2$ -congruent (here  $\mathbb{Z}^2$ -congruent means that two M-triangles can be mapped into each other by a  $\mathbb{Z}^2$ -symmetry); (ii) there are  $N_1 > 1$  M-triangles, and they are not  $\mathbb{R}^2$ -congruent; (iii) a mixture of (i) and (ii). Cf. Fig. 9. The value  $K$  is the number of non- $\mathbb{Z}^2$ -congruent M-triangles. Next: (a)  $m_k = 1$  if  $D^2 = 2$ , and (b)  $m_k = 2$  or  $4$  when  $D^2 > 2$  and the M-triangle  $\triangle$  defining the PGS-equivalence class is isosceles or not, respectively. See Theorems 1 (i), 2 and sections 3.1, 3.2 in [27].

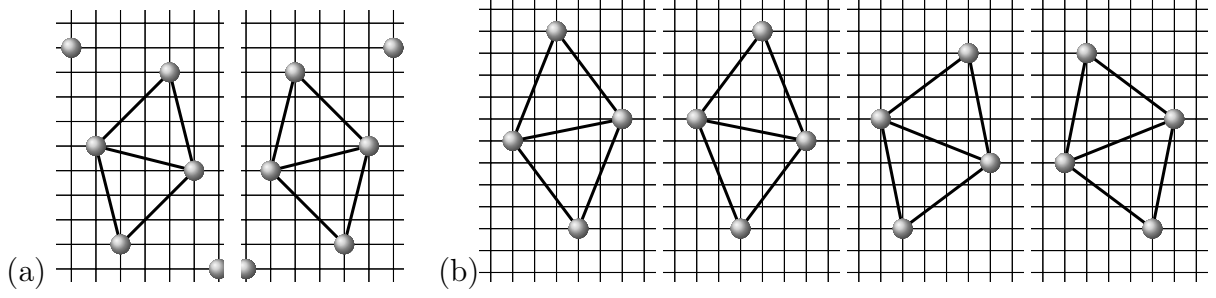


Figure 8: PGSs on  $\mathbb{Z}^2$  for (a)  $D^2 = 16$ ,  $S = 15$  and (b)  $D^2 = 25$ ,  $S = 23$ . In both cases, the M-triangles are  $\mathbb{Z}^2$ -congruent, and there is a single PGS-equivalence class. Consequently,  $K = 1$ . For  $D^2 = 16$  the M-triangles are isosceles, and there are 2 MDA-sub-lattices. For  $D^2 = 25$  the M-triangles are non-isosceles, and there are 4 MDA-sub-lattices. Accordingly,  $\sigma = 15$ ,  $m = 2$  for  $D^2 = 16$  and  $\sigma = 23$ ,  $m = 4$  for  $D^2 = 25$ . The number of PGSs is 30 and 92, respectively.

Similarly to  $\mathbb{A}_2$  and  $\mathbb{H}_2$ , the identification of PGSs on  $\mathbb{Z}^2$  is intrinsically connected with algebraic number theory. It turns out that, for a given  $D$ , one can characterize the corresponding M-triangles via solutions to *norm equations* in ring  $\mathbb{Z}[\sqrt[6]{-1}]$  (i.e., the ring of algebraic integers in the cyclotomic field generated by  $\zeta_{12} = e^{\pi i/6}$ ). Such a connection helps to prove that uniqueness of an M-triangle and each of non-uniqueness types (i)–(iii) occur for infinitely many values  $D$ , and the degrees of degeneracy  $N_0$ ,  $N_1$  can be arbitrarily large as  $D \rightarrow \infty$ . See Theorem 3 in [27].

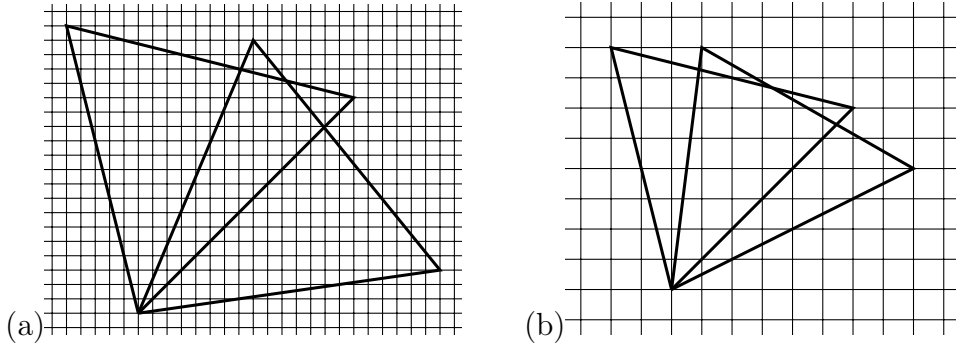


Figure 9: Non-uniqueness of M-triangles on  $\mathbb{Z}^2$ : (a) for  $D^2 = 425$ ,  $S = 375$  ( $\mathbb{R}^2$ - but not  $\mathbb{Z}^2$ -congruent,  $N_0 = 2$ ) and (b) for  $D^2 = 65$ ,  $S = 60$  ( $\mathbb{R}^2$ -non-congruent,  $N_1 = 2$ ). Which PGS-class generates EGDs is determined by dominance.

**3.6.** It is possible to check that any non-periodic ground state on  $\mathbb{Z}^2$  contains at least one infinite connected component of non-M-triangles and no finite ones. Moreover, the number of non-M-triangles in a  $\mathbb{Z}^2$ -square  $\mathbb{V}(L)$  of side-length  $L$  can only grow at most linearly with  $L$ ; this means that in a non-periodic ground state, non-M-triangles form, effectively, a one-dimensional array.

A similar pattern for non-periodic ground states emerges on  $\mathbb{A}_2$  and  $\mathbb{H}_2$ . Let us repeat once more that non-periodic ground states do not generate EGDs in dimension two [10]. Cf. discussions in section 3.1.

## 4 The Peierls bound

**4.1. Contours.** Contours play a central role in the P-S theory. Physically speaking, contours describe local perturbations of PGSs. They emerge when we (i) remove some particles from a PGS  $\varphi$  and (ii) add some new particles at ‘inserted’ sites, maintaining  $D$ -admissibility.

A formal definition is as follows. First, we define a *template* as a parallelogram spanned by two non-collinear vectors such that each MDA sub-lattice is invariant under shifts by both of these vectors. Typically we choose a parallelogram with a minimal area and a maximal acute angle. Cf. Fig. 10.

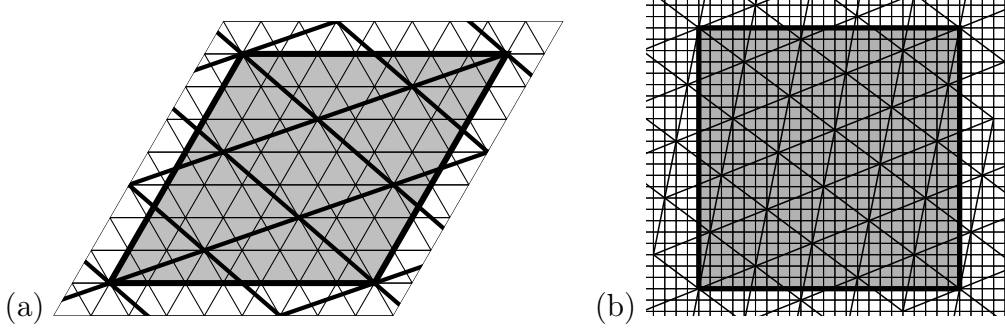


Figure 10: Templates (gray) and fundamental parallelograms on  $\mathbb{A}_2$  for  $D^2 = 7$  (a) and on  $\mathbb{Z}^2$  for  $D^2 = 25$  (b).

We say that a template  $F$  is  $\varphi$ -regular in  $\phi$  if,  $\forall x \in F$ , we have  $\phi(x) = \varphi(x)$ . A template  $F$  is called  $\varphi$ -correct if  $F$  and all 8 of its adjacent templates are  $\varphi$ -regular. The *frustrated set* is formed by the union of templates that are not  $\varphi$ -correct  $\forall \varphi \in \mathcal{P}(D)$ .

A contour  $\Gamma$  in a  $D$ -AC  $\phi \in \mathcal{A}(D)$  is defined as a pair  $(S, \phi|_S)$  where  $S = \text{Supp}(\Gamma) \subset \mathbb{W}$  is a connected component of the frustrated set. We say that  $\Gamma$  is finite if the set  $\text{Supp}(\Gamma)$  is finite.

Let  $\Gamma$  be a finite contour in a  $D$ -AC  $\phi \in \mathcal{A}(D)$ . The complement  $\mathbb{W} \setminus \text{Supp}(\Gamma)$  has one infinite connected component which we call the *exterior* of  $\Gamma$  and denote by  $\text{Ext}(\Gamma)$ . In addition, set  $\mathbb{W} \setminus \text{Supp}(\Gamma)$  may have finitely many *interior* connected components; they are denoted by  $\text{Int}_j(\Gamma)$ ,  $j = 1, \dots, J$ , and we set  $\text{Int}(\Gamma) = \bigcup_{j=1}^J \text{Int}_j(\Gamma)$ . Cf. Fig. 11. We say that  $\Gamma$  is a  $\varphi$ -contour in  $\phi$  if every template  $F \subset \text{Ext}(\Gamma)$  adjacent to  $\text{Supp}(\Gamma)$  is  $\varphi$ -correct in  $\phi$ . We say that  $\Gamma$  is an *external* contour in  $\phi$  if  $\text{Supp}(\Gamma)$  does not lie in  $\text{Int}(\Gamma')$  for any other contour  $\Gamma'$ .

An important point is that a contour can be considered without a reference to the AC  $\phi$ : it is enough that we indicate (i) a  $D$ -AC  $\psi_\Gamma$  over set  $\text{Supp}(\Gamma)$ , (ii) an external phase  $\varphi$  and the internal phases  $\varphi_j$ , such that every template  $F \subset \text{Ext}(\Gamma)$  adjacent to  $\text{Supp}(\Gamma)$  is  $\varphi$ -correct and every template  $F \subset \text{Int}_j(\Gamma)$  adjacent to  $\text{Supp}(\Gamma)$  is  $\varphi_j$ -correct,  $j = 1, \dots, J$ .

With the above definitions at hand, we write down the contour representation for the partition function:

$$Z(\mathbb{V}_n || \varphi) = u^{\sharp(\varphi|_{\mathbb{V}_n})} \sum_{\{\Gamma_i\} \subset \mathbb{V}_n} \prod_i w(\Gamma_i). \quad (6)$$

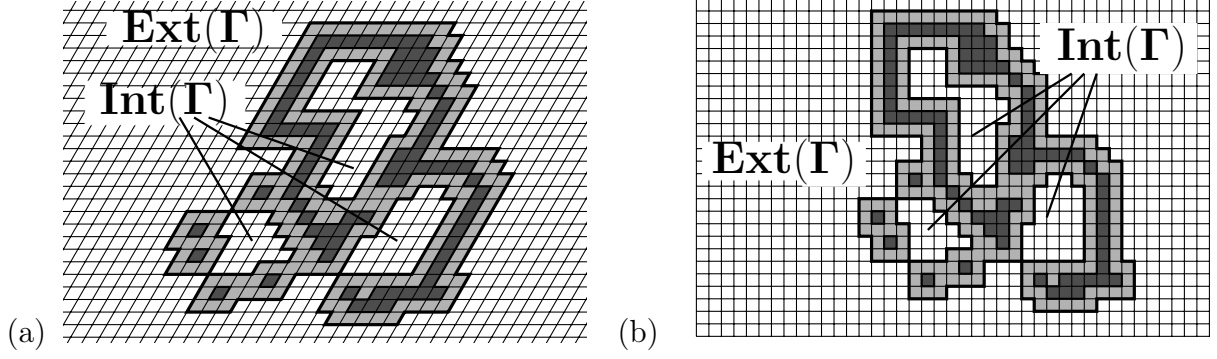


Figure 11: Contour supports on  $\mathbb{A}_2/\mathbb{H}_2$  (a) and  $\mathbb{Z}^2$  (b). Dark-gray color marks non-correct templates, light-gray templates are their neighbors. Note that both dark-gray and light-gray templates are non-correct, and the difference between the two types is that dark-gray are also non-regular, while the light-gray are regular.

Here the summation goes over *compatible* contour collections  $\{\Gamma_i\}$  with pair-wise disjoint  $\text{Supp}(\Gamma_i) \subset \mathbb{V}_n$ , while  $w(\Gamma)$  stands for the *statistical weight* of contour  $\Gamma$ :

$$w(\Gamma) = u^{\#(\psi_\Gamma) - \#(\varphi \upharpoonright_\Gamma)}. \quad (7)$$

Pictorially, compatibility means that if two of contours,  $\Gamma$  and  $\Gamma'$ , from the collection are not separated by a third contour  $\bar{\Gamma}$  then their external and/or internal phases are coordinated. Formally, it requires two properties. (a) If (i)  $\text{Supp}(\Gamma') \subset \text{Int}_j(\Gamma)$  and (ii) there is no contour  $\bar{\Gamma}$  in  $\{\Gamma_i\}$  with  $\text{Supp}(\Gamma') \subset \text{Int}(\bar{\Gamma})$  and  $\text{Supp}(\bar{\Gamma}) \subset \text{Int}_j(\Gamma)$  then the internal phase  $\varphi_j$  of  $\Gamma$  serves as the external phase for  $\Gamma'$ . (b) If (i)  $\text{Supp}(\Gamma') \subset \text{Ext}(\Gamma)$  and (ii) there is no contour  $\bar{\Gamma}$  in  $\{\Gamma_i\}$  with  $\text{Supp}(\bar{\Gamma}) \subset \text{Ext}(\Gamma)$  and  $\text{Supp}(\Gamma') \subset \text{Int}(\bar{\Gamma})$  then  $\Gamma$  and  $\Gamma'$  have the same external phase. Note that all external contours in a compatible collection  $\{\Gamma_i\}$  are  $\varphi$ -contours for the same  $\varphi$ . Here we refer to a  $\varphi$ -contour when the external phase of the contour coincides with  $\varphi$ , i.e., all corresponding external light-gray squares in Fig. 11 are  $\varphi$ -correct.

The condition upon  $\mathbb{V}_n$  in (6) is that  $\mathbb{V}_n$  is a finite union of templates.

We then can think of a Gibbs distribution  $\mu_{\mathbb{V}_n}(\cdot \| \varphi)$  as a probability measure on compatible contour collections  $\{\Gamma_i\}$  in  $\mathbb{V}_n$ .

#### 4.2. The Peierls constant. The next step is to establish a bound

$$\#(\psi_\Gamma) - \#(\varphi \upharpoonright_\Gamma) \leq -p \|\text{Supp}(\Gamma)\|. \quad (8)$$

Here  $\|\text{Supp}(\Gamma)\|$  stands for the number of templates in  $\text{Supp}(\Gamma)$  and  $p = p(D, \mathbb{W}) > 0$  is a *Peierls constant* per a template. Then the statistical weight  $w(\Gamma)$  will obey  $w(\Gamma) \leq u^{-p \|\text{Supp}(\Gamma)\|}$ , and a standard Peierls argument will lead to properties **(P1-5)** below.

By the definition of a contour, every template  $F \subset \text{Supp}(\Gamma)$  contains some sort of a defect. A trivial defect is when at least one particle can be added to configuration  $\psi_\Gamma \upharpoonright_F$ ; in this case we get at least a factor 1 in place of  $p$  in inequality (8).

For a saturated defective template  $F \subset \text{Supp}(\Gamma)$ , the situation is more complex. Here we use the *Delaunay triangulation* for  $\psi_\Gamma \upharpoonright_F$ ; the fact is that for each of the triangles the

area is  $\geq \sigma/2$ , and for at least one triangle the area is  $\geq (1 + \sigma)/2$ . (Note that the lattice triangle has a half-integer area.) The number of such triangles is  $O(\|\text{Supp}(\Gamma)\|)$ . On the other hand, the number of particles inside  $\text{Supp}(\Gamma)$  is twice the number of triangles. This ultimately leads to (8).

The constant  $p(D)$  can actually be lower-bounded by  $c/D^2$ .

## 5 Dominance, extreme Gibbs distributions

**5.1.** If for a given  $D$ , the number  $\#\mathcal{E}(D, \mathbb{W})$  of PGS-equivalence classes equals 1, then for  $u$  large enough the number of EGDs equals the number  $\#\mathcal{P}(D, \mathbb{W})$  of PGSs. When the number of PGS-equivalence classes  $K$  is greater than 1, i.e., there are multiple PGS-equivalence classes, not all PGS-classes generate EGDs. In a sense, it is an expected behavior since an absence of explicit symmetry between the representatives of different PGS-equivalence classes results in different sets of their perturbations (contours). The PGSs generating EGDs are referred to as stable/dominant ones. The dominant classes are those which minimize a ‘truncated free energy’ for the ensemble of small contours; cf. [36]. Observe that typically in the P-S theory the statistical weight of a contour decreases exponentially with the size of the contour. Accordingly, the contours can be listed in the decreasing order of their statistical weights; geometrically smaller contours appear earlier in the list. A truncated free energy emerges when we discard the contours whose statistical weight is lower than a given threshold value.

We conjecture that for the H-C model the dominant PGS-equivalence class is always unique, since otherwise there would be too many additional hidden symmetries.

**5.2.** As an outcome of the P-S theory for the H-C model we have the following properties.

**(P1)** Each EGD  $\mu \in \mathcal{E}(D, \mathbb{W})$  is generated by a PGS. That is, each EGD is of the form  $\mu_\varphi$  for some  $\varphi \in \mathcal{P}(D, \mathbb{W})$ . If PGSs  $\varphi_i$  generate EGDs  $\mu_{\varphi_i}$ ,  $i = 1, 2$ , and  $\varphi_1 \neq \varphi_2$  then  $\mu_{\varphi_1} \perp \mu_{\varphi_2}$ . The EGDs inherit symmetries from the PGSs.

**(P2)** Consequently, EGD-generation is a class property: if a PGS  $\varphi \in \mathcal{P}(D, \mathbb{W})$  generates an EGD  $\mu_\varphi$  then every PGS  $\varphi'$  from the same equivalence class generates an EGD  $\mu_{\varphi'}$ . Such a class is referred to as dominant. Obviously, if a PGS-equivalence class is unique, it is dominant.

**(P3)** Each EGD  $\mu_\varphi$  exhibits the following properties. For  $\mu_\varphi$ -almost all  $\phi \in \mathcal{A}$ : (i) all contours  $\Gamma$  in  $\phi$  are finite, (ii) for any site  $x \in \mathbb{W}$  there exist only finitely many contours  $\Gamma$  (possibly none) such that  $x$  lies in the interior of  $\Gamma$ , (iii) there are countably many disjoint  $D$ -connected sets of  $\varphi$ -correct templates, one of which is infinite while all remaining  $D$ -connected sets are finite, (iv) for every  $\varphi' \in \mathcal{P}(D, \mathbb{W}) \setminus \{\varphi\}$ , there are countably many  $D$ -connected sets of  $\varphi'$ -correct templates all of which are finite.

**(P4)** EGD  $\mu_\varphi$  admits a polymer expansion and has an exponential decay of correlations.

**(P5)** As  $u \rightarrow \infty$ ,  $\mu_\varphi$  converges weakly to a measure sitting on a single  $D$ -AC  $\varphi$ .

Property **(P3)** establishes a percolation picture for EGD  $\mu_\varphi$ : there is a ‘sea’ of  $\varphi$ -correct templates with ‘islands’ of non- $\varphi$ -correct sites inside which there may be ‘lakes’ of



templates of different correctness, etc. In such a picture, contours mark ‘coastal/shallow-water strips’.

**5.3.** Specification of dominant PGS-classes for a general value  $D$  remains an open question; in [26], Theorems 4, 5, 6, 10, we present a complete answer for values  $D^2 = 49, 147, 169$  on  $\mathbb{A}_2$  or  $\mathbb{H}_2$  by classifying small contours. We expect that a similar approach could be used for other examples.

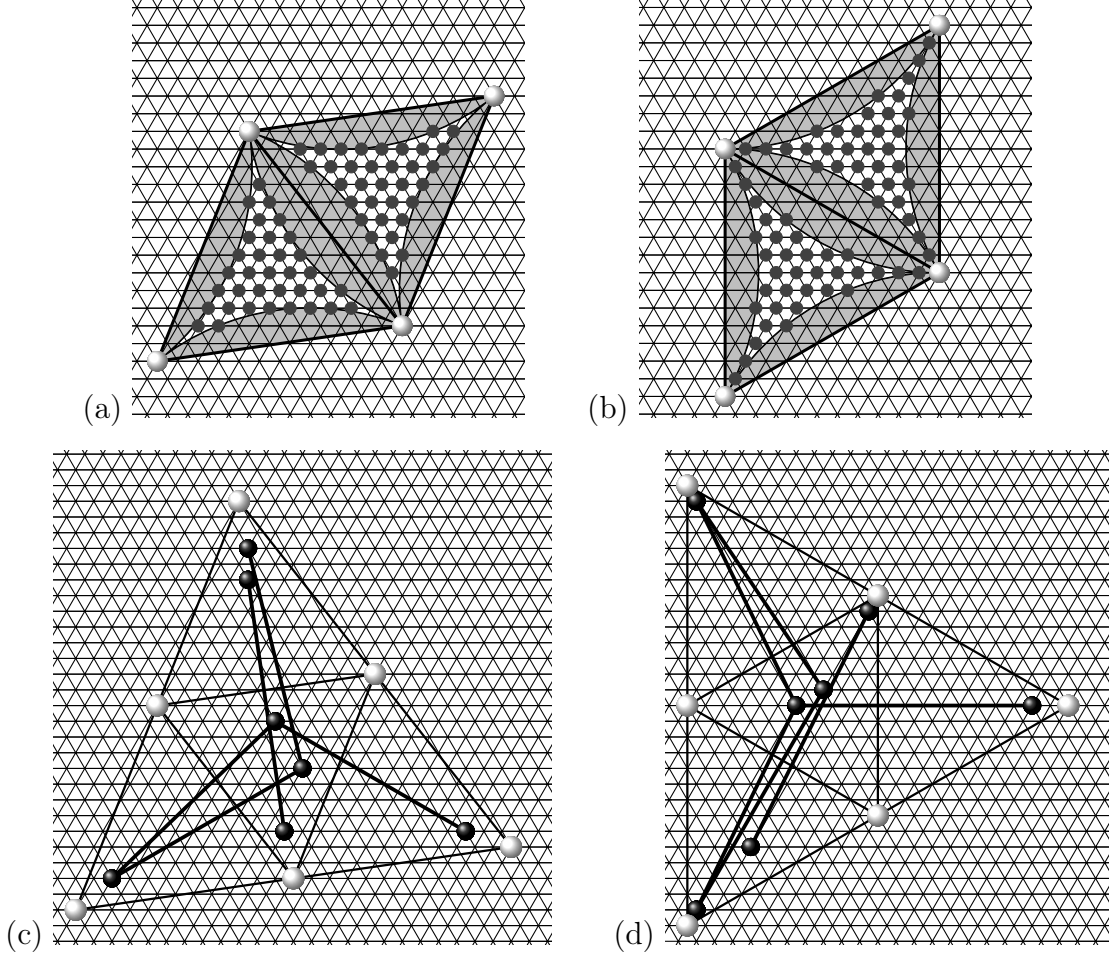


Figure 12: Dominance on  $\mathbb{A}_2$ , for  $D^2 = 147$ . This figure shows admissible  $u^{-2}$ -insertions for  $D^2 = 147$  on  $\mathbb{A}_2$ . Here we have two PGS-equivalence classes, one ‘inclined’ (a, c) and one ‘vertical’ (b, d). Single admissible  $u^{-2}$ -insertions are marked by dark dots (a, b); gray lenses indicate areas from where a single insertion repels four sites in a PGS and hence yields a  $u^{-2}$ -insertion. The number of single  $u^{-2}$ -insertions is 68 per a  $D$ -rhombus for both PGS-classes. Double and triple  $u^{-2}$ -insertions are shown on frames (c, d) and a quadruple insertion on frame (d). For the inclined class there is no admissible quadruple  $u^{-2}$ -insertion, and for the neither class there is an admissible  $n$ -particle  $u^{-2}$ -insertion with  $n \geq 5$ . The count of all  $u^{-2}$ -insertions shows that the vertical PGS-class is dominant (an argument presented in [26], sections 6, 7, shows that contributions of order  $u^{-3}$  and higher are irrelevant in the case under consideration).

The simplest small contour occurs when we merely remove a particle from a PGS  $\varphi$ . Clearly, all PGSs are ‘equal in rights’ relative to this perturbation type, as they are maximally-dense. The same is true about removing pairs of particles, etc. Then there is a possibility of inserting one and removing three particles, at the vertices of the Delaunay triangle of  $\varphi$ ; these are single insertions. Note that inserting a single particle implies removing at least three. Continuing, we can think of double insertions where pairs of inserted particles remove four particles at the vertices of covering parallelogram in  $\varphi$ , and so on, maintaining the difference 2 between the number of removed and inserted particles (and, of course,  $D$ -admissibility). This yields a finite collection of admissible  $u^{-2}$ -insertions where we add  $n$  and remove  $n + 2$  particles.

In the above-mentioned examples, we (a) enumerate the  $u^{-2}$ -insertions, and (b) verify that higher-order insertions (beginning with  $u^{-3}$ ) can be discarded when fugacity  $u$  is large enough. Task (b) is achieved via standard polymer expansion techniques. Accordingly, the free energy of the model under consideration is represented as an absolutely convergent polymer series, where the polymers are connected unions of contours. The amount of such objects of size  $n$  is upper-bounded by  $C^n$ , where  $C$  is an absolute constant and  $n$  is the number of the lattice sites in a polymer. On the other hand, the absolute value of the statistical weight of a polymer is upper-bounded by  $u^{-pn}$ , where  $p$  is the Peierls constant from (8). Therefore, the polymer expansion converges for large  $u$  as soon as  $u^{-p}C < 1$ . Moreover, for all  $u > 2C^{1/p}$  there exists  $n_0$  such that the tail of the polymer series (with  $n \geq n_0$ ) does not exceed  $u^{-3} \ll u^{-2}$  in the absolute value. The remaining initial part of the series does not contain more than  $C^{2n_0}$  terms. For  $u > C^{4n_0}$  the total contribution of terms with the statistical weight less than or equal to  $u^{-3}$  does not exceed  $u^{-3}C^{2n_0} < u^{-2.5} \ll u^{-2}$ .

This way the problem is reduced to task (a): enumeration of the  $u^{-2}$ -insertions. The most involved part (requiring a computer-assisted proof) is to check that the maximal number of added particles in admissible  $u^{-2}$ -insertions is  $n = 4$ : here we remove 6 occupied sites from the boundary of a  $2D$ -triangle in a given PGS; cf. Fig. 12 (d) for  $D^2 = 147$ . Generally, a Peierls bound implies that all  $u^{-2}$ -insertions have bounded size depending on the corresponding constant  $p$ . The problem is that  $p$  is relatively small, and the corresponding bound is impractically large. The fact that there is no insertion of  $n \geq 5$  particles implying the removal of at most  $n + 2$  particles requires an additional argument. See [26], Lemmas 7.1–7.3.

The above approach allows us to identify the dominant PGS-classes for  $D^2 = 49, 147, 169$  on  $\mathbb{A}_2$  and  $\mathbb{H}_2$ .

## 6 Conclusions

In this work we construct the phase diagram for the hard-core model on  $\mathbb{A}_2$ ,  $\mathbb{H}_2$  and  $\mathbb{Z}^2$  in a high-density/large-fugacity regime for all non-sliding values of the exclusion distance  $D$  or, equivalently, for any label  $k$  of excluded neighbors. These results are rigorously established in the thermodynamic limit. The H-C model in this regime admits a straightforward application of the P-S theory, but the challenge here lies in determining the periodic ground states and verifying a suitable Peierls bound. A zest of the work is that the PGSs have been identified by means of algebraic number theory. Since the PGSs

coincide with periodic disk-packings of maximal density, we also obtain the description of the latter, which yields a solution to the disk-packing problem on  $\mathbb{A}_2$ ,  $\mathbb{H}_2$  and  $\mathbb{Z}^2$  for all disk diameters  $D > 0$ .

In particular, the complete structure of the large fugacity-phase diagram has been established when there is a single PGS-equivalence class. Also, it has been proven that there are only finitely many sliding values of  $D$ , and all of them have been identified.

The work also highlights open problems beyond the P-S theory. (1) How to identify the dominant class(es) among multiple PGS-equivalence classes? (2) What is the phase diagram as a function of  $u > 0$  for a given value of  $D$ ? (3) What is the dependence of the critical value(s) of  $u$  upon  $D$ ? If point  $u^0 = u^0(D)$  separates the uniqueness and non-uniqueness domains, and  $u^1(D)$  is the lower threshold for the large-fugacity regime, then do we have  $u^0(D) = u^1(D)$  for some/all/no  $D$ ? In other words, is there one or several phase transitions for a given  $D$  and what is the type of the transition(s)? (3) Could our results provide hints towards understanding the model in  $\mathbb{R}^2$ ? The challenge here is that our technique is applicable for  $u > u^0(D)$ , where  $u^0(D)$  increases to  $\infty$  as  $D \nearrow \infty$ .

A natural next step is to consider the HC model on  $\mathbb{Z}^3$ . Here the situation is more complex, mainly due to its close relationship with the Kepler conjecture. Nevertheless, similar P-S theory based results have been rigorously obtained in [28] for certain special values of  $D$ :  $D^2 = 2, 3, 4, 5, 6, 8, 9, 10, 12, 2\ell^2$  where  $\ell \in \mathbb{Z}$ . Also see [21], [35].

**Acknowledgement.** IS and YS thank the Math Department, Penn State University, for support during this work. YS thanks St John's College, Cambridge, for support. The authors express their gratitude to the referees for numerous useful remarks and suggestions.

## References

- [1] Akimenko, S.S., Gorbunov, V.A., Myshlyavtsev, A.V. and Stishenko, P.V. The renormalization group study of hard-disk model on a triangular lattice. *Phys. Rev. E* **100** (2019), 022108
- [2] Akimenko, S., Myshlyavtsev, A., Myshlyavtseva, M., Gorbunov, V., Podgornyi, S. and Solovyeva, O. Triangles on triangular lattice: insights into self-assembly in two dimensions driven by shape complementarity. *Phys. Rev. E* **105** (2022), 044104
- [3] Baxter, R.J. Hard hexagons: exact solution. *J. Phys. A.* **13** (1980), L61
- [4] Baxter, R.J. Planar lattice gases with nearest-neighbor exclusion. *Ann. Comb.* **3** (1999), 191–203
- [5] Bricmont, J. *Making sense of Statistical mechanics*. Cham, Switzerland: Springer Nature, 2022
- [6] Burley, D.M. A lattice model of a classical hard sphere gas. *Proc. Phys. Soc.* **75** (1960), 262-274; **77** (1961), 451-458

- [7] Connelly, R. and Dickinson, W. Periodic planar disc packings. *Phil. Trans. Roy. Soc.*, **A372**, 20120039. <http://dx.doi.org/10.1098/rsta.2012.0039>
- [8] Dobrushin, R. The problem of uniqueness of a Gibbsian random field and the problem of phase transitions. *Funct. Anal. Appl.* **4**:4 (1968), 302–312
- [9] Darjani, S., Koplik, J., Banerjee, S. and Pauchard, V. Liquid-hexatic-solid phase transition of a hard-core lattice gas with third neighbor exclusion. *J. Chem. Phys.* **151** (2019), 104702
- [10] Dobrushin, R. and Shlosman, S. The problem of translation invariance of Gibbs states at low temperatures. In: *Math. Phys. Reviews*, **5**, pp. 53–195. Harwood Academic Publ., 1985
- [11] Fernandes, H.C.M., Arenzon, J.J. and Levin, Y. Monte carlo simulation of two-dimensional hard core lattice gases. *J. Chem. Phys.* **126** (2007), 114508
- [12] Friedli, S. and Velenik, Y. *Statistical mechanics of lattice systems: a concrete mathematical introduction*. Cambridge: Cambridge University Press, 2017
- [13] Gaunt, D.S. and Fisher, M.E. Hard-sphere lattice gases, I. Plane-square lattice. *J. Chem. Phys.* **43** (1965) 2840–2863
- [14] Gaunt, D.S. Hard-sphere lattice gases, II. Plane-triangular and three-dimensional lattices. *J. Chem. Phys.* **46** (1967) 3237–3259
- [15] Georgii, H.-O. *Gibbs measures and phase transitions*. New York: Springer, 1990.
- [16] Georgii, H.O, Haggstrom, O., Maes, C. The random geometry of equilibrium phases. In: *Phase Transitions and Critical Phenomena*, **18**, Elsevier, 2001, 1-142.
- [17] Hadas, D. and Peled, R. Columnar order in random packings of  $2 \times 2$  squares on the square lattice. arXiv:2206.01276v1 (2022)
- [18] Heilmann, O. and Praestgaard, E. Phase transition of hard hexagons on a triangular lattice. *J. Stat. Phys.* **9** (1973), 1–22
- [19] Ireland K. and Rosen, M. *A classical introduction to modern number theory*. Berlin/New York: W. de Gruyter, 2011.
- [20] Jaleel, A.A., Mandal, D., Thomas, J.E. and Rajesh, R. The freezing phase transition in hard core lattice gases on triangular lattice with exclusion up to seventh next-nearest neighbor. arXiv:2206.04985v1, (2022)
- [21] Jaleel, A.A., Thomas, J.E., Mandal, D., Sumedha and Rajesh, R. Rejection-free cluster Wang-Landau algorithm for hard-core lattice gases. *Phys. Rev. E* **104** (2021), 045310
- [22] Jauslin, I. and Lebowitz, J. Crystalline ordering and large fugacity expansion for hard core lattice particles. *J. Phys. Chem. B* **122** **13** (2017), 3266–3271

- [23] Jauslin, I. and Lebowitz, J. High-fugacity expansion, Lee-Yang zeros and order-disorder transitions in hard-core lattice systems. *Comm. Math. Phys.* **364** (2018), 655–682
- [24] Krachun, D. Triangles on  $\mathbb{Z}^2$  and sliding phenomenon. arXiv:1912.07566v1 (2019)
- [25] Krachun, D. Extreme Gibbs measures for high-density hard-core model on  $\mathbb{Z}^2$ . arXiv:1912.07566v2 (2020)
- [26] Mazel, A., Stuhl, I. and Suhov, Y. High-density hard-core model on triangular and hexagonal lattices. arXiv:1803.04041v2 (2020)
- [27] Mazel, A., Stuhl, I. and Suhov, Y. High-density hard-core model on  $\mathbb{Z}^2$  and norm equations in ring  $\mathbb{Z}[\sqrt[6]{-1}]$ . arXiv:1909.11648v2 (2020)
- [28] Mazel, A., Stuhl, I. and Suhov, Y. Kepler’s conjecture and phase transitions in the high-density hard-core model on  $\mathbb{Z}^3$ . arXiv:2112.14250v1 (2021)
- [29] Nath, T. and Rajesh, R. Multiple phase transitions in extended hard-core lattice gas models in two dimensions. *Phys. Rev. E* **90** (2014), 012120
- [30] Nath, T. and Rajesh, R. The high density phase of the  $k$ -nn hard core lattice gas model. *J. Stat. Mech.* (2016), 073203
- [31] Pirogov, S. and Sinai, Y. Phase diagrams of classical lattice systems. *Teor. Mat. Fiz.* **25**, **26** (1975, 1976), 1185–1192, 61–76
- [32] Sinai, Ya.G. *Theory of phase transitions: rigorous results*. Oxford: Pergamon Press, 1982
- [33] Slawny, J. Low temperature properties of classical lattice systems: phase transitions and phase diagrams. In: *Phase transitions and critical phenomena*. vol. **11**, New York: Academic Press, (1987), 127-205
- [34] Thewes, F.C. and Fernandes, C.M. Phase transitions in hardcore lattice gases on the honeycomb lattice. *Phys. Rev. E* **101** (2020), 062138
- [35] Vigneshwar, N., Mandal, D., Damle, K., Dhar, D. and Rajesh, R. Phase diagram of a system of hard-cubes on the cubic lattice. *Phys. Rev. E* **99** (2019), 052129
- [36] Zahradnik, M. An alternate version of in the context-Sinai theory. *Comm. Math. Phys.*, **93** (1984), 559–581
- [37] Zahradnik, M. A short course in the Pirogov-Sinai theory. *Rendiconti Mat. Appl.*, **18** (1998), 411–486